Bézier Description of Space Trajectories

Francesco de Dilectis,* Daniele Mortari,†

Texas A&M University, College Station, Texas

and Renato Zanetti‡

NASA Jonhson Space Center, Houston, Texas

I. Introduction

This study introduces a new method to estimate spacecraft trajectories using non-rational Bézier functions to fit a set of measured positions. These implicit functions are defined by a set of control points that, in general, do not belong to the trajectory. The values of the implicit parameters, the control points, and the Bézier function degree are estimated by an iterative least-squares process. The main advantage of this approach is that *it does not require dynamics and perturbations models*, and it provides not only a best fitting of the trajectory, but also associates interpolated points with corresponding times. This approach proves particularly useful either when dynamics and/or perturbations are difficult to model (e.g., solar pressure depending on solar activities and attitude) or when unpredictable events (e.g., pipe leak) make the expected dynamics model inaccurate. To validate the proposed approach, comparison with Iterative Batch Least Squares and Extended Kalman Filter is provided for three segments of a cislunar trajectory. The basic inspiration for this method comes from the observation that Gooding's initial orbit determination method[3] provides, in general, better performances than most alternative methods. This is because Gooding's method is based on the Lambert problem, which is a known Two-Point Boundary Value Problem (TPBVP), while most of the other methods fall into the Initial Value Problem (IVP) category. In general, IVP's are easier to solve than TPBVP's, but the solutions are usually more sensitive to uncertainties in the data. This is because to solve an IVP all

*PhD Graduate Student, 301B Reed McDonald, Aerospace Engineering, Texas A&M University, College Station, TX 77843-3141. E-mail: f.de.dilectis@neo.tamu.edu

†Professor, 746C H.R. Bright Bldg, Aerospace Engineering, Texas A&M University, College Station, TX 77843-3141, AAS Fellow, AIAA Associate Fellow. E-mail: mortari@tamu.edu

‡GN&C Autonomous Flight Systems Engineer, Aeroscience and Flight Mechanics Division, EG6, 2101 NASA Parkway. NASA Johnson Space Center, Houston, Texas 77058. AIAA Senior Member.

information is given at one point. On the other hand a TPBVP relies on information provided at two distinct points, initial and final. This makes them usually more accurate and, more importantly, less sensitive to small perturbations of the data. Bézier functions are uniquely described by a set of coefficients called "control points". For this reason trajectories described by these functions are not very sensitive to uncertainty: the power of Bézier functions is that the information is "distributed" along the trajectory.

The method proposed in this study is independent from the physics involved, relying only on observations. Compared to other families of implicit functions, like B-splines, Bézier polynomials can be rewritten in a linear form that greatly simplifies the optimization problem, as explained below. Moreover, this approach not only performs best fitting of a trajectory, but also associates points of the curve with measurement times by best-fitting time with a Bézier curve found independently from the interpolated trajectory, but related to it by the curvilinear parameter. Validation has been performed via estimation of a cislunar trajectory using visual camera measurements which in turn has been simulated and with NASA-GMAT. However the proposed method is applicable to different scenarios as long as an estimated set of position vectors and associated times are available.

II. Trajectory Estimation using Non-Rational Bézier Functions

Expanding on previous developments,[4] a Bézier function can be written as a linear combination of Bernstein polynomials,

$$\boldsymbol{r} = \sum_{k=0}^{n} \boldsymbol{c}_k B_k^n(s) \quad \text{where} \quad B_k^n(s) = \binom{n}{k} s^k (1-s)^{n-k}, \quad s \in [0,1]. \tag{1}$$

Where $\boldsymbol{c}_k$ are the control points in 3D and s is the implicit parameter with no physical meaning. By use of the binomial theorem, any non-rational Bézier function can be written as:

$$\boldsymbol{r} = \sum_{k=0}^{n} \left\{ \boldsymbol{c}_k \binom{n}{k} \left[\sum_{j=0}^{n-k} \binom{n-k}{j} (-1)^{n-(k+j)} s^{n-j} \right] \right\}. \tag{2}$$

While Eq. (2) itself is rather cumbersome, by considering m points along the curve and the corresponding values of the parameter s, $\{s_1, \ldots, s_m\}$, we obtain a system of linear equations in $\boldsymbol{c}_k$ which can be rewritten in a much more compact form:

$$\underset{3\times m}{R} = \underset{3\times(n+1)}{C} \; \underset{(n+1)\times(n+1)}{M} \; \underset{(n+1)\times m}{S} \tag{3}$$

where

$$
\begin{cases} R = [\,\boldsymbol{r}_1,\ \boldsymbol{r}_2,\ \ldots,\ \boldsymbol{r}_m\,] \\ \\ C = [\,\boldsymbol{c}_0,\ \boldsymbol{c}_1,\ \ldots,\ \boldsymbol{c}_n\,] \end{cases} \quad \text{and} \quad S = \begin{bmatrix} 0 & s_2^n & s_3^n & \cdots & s_{m-2}^n & s_{m-1}^n & 1 \\ 0 & s_2^{n-1} & s_3^{n-1} & \cdots & s_{m-2}^{n-1} & s_{m-1}^{n-1} & 1 \\ \vdots & \vdots & \vdots & \ddots & \vdots & \vdots & \vdots \\ 0 & s_2 & s_3 & \cdots & s_{m-2} & s_{m-1} & 1 \\ 1 & 1 & 1 & \cdots & 1 & 1 & 1 \end{bmatrix} \tag{4}
$$

and the elements of matrix M are of the form $M_{i,j} = \binom{n}{i}\binom{n-i}{j}(-1)^{n-(i+j)}$, $i = 0, \ldots, n$, $j = 0, \ldots, n-i$ (to keep the numbering consistent with the control points, in this formalism the first element of the M matrix is $M_{0,0}$, and so on). It follows easily from the properties of binomial coefficients that $m_{i,j} = m_{j,i}$, and also $m_{i,j} = 0$ whenever $i + j > n$. Matrix C can be obtained from Eq. (3) using Least Squares:

$$
C = R\,S^{\mathrm{T}}\,(SS^{\mathrm{T}})^{-1}\,M^{-1} \tag{5}
$$

Solving Eq. (5) requires a choice for the degree n and the parameter distribution. To find the optimal values, in the sense of minimizing a given error measure, two iterative processes are used in sequence, one to establish the degree and one for the parameter.

Because all but the simplest trajectories have variable curvature, and small values of curvature are often hidden by noise, it is not possible to define *a priori* the optimal degree to use in a specific application. In general, trajectories with more variable curvature are better approximated by polynomials of higher degree. On the other hand, the maximum degree usable for a given segment is limited by the number of data points available, according to:

$$
n = \left\lceil \frac{m}{3} - 1 \right\rceil . \tag{6}
$$

This condition must be satisfied to guarantee that the linear system is not undetermined. However, this is just an upper limit for the range in which the algorithm can search for the optimal degree, and not a condition to be enforced as the number of measurement accrued increases. In fact, a stricter limit on the degree is imposed by numerical reasons as matrix S becomes progressively ill-conditioned for increasing values of n, becoming finally unstable around $n \simeq 10$, as found experimentally. Therefore, to find the optimal degree, the algorithm starts approximating the data with a polynomial of degree 2 and then increases this value until an appropriately chosen measure of the error reaches a local minimum, or the degree reaches either of the limits introduced above, whichever is smaller. In most cases, the optimal degree found iteratively will be close or equal to the maximum defined by Eq. (6). Thus, that while currently there are limits to the maximum degree achievable with this method, this does not reflect negatively on the ability of the curve to interpolate the data, for the applications here considered.

A. Bézier Parameters Least Squares optimization

To solve Eq. (5), a distribution of the parameter s corresponding to the measurements has to be assumed. If the data is provided at constant time step, a uniform distribution can be used:

$$s_k = \frac{k-1}{n-1} \qquad \text{where} \qquad k \in [1, m]. \tag{7}$$

Another valid approximation relates the distribution with the relative distance of subsequent data points, as per the following:

$$\begin{cases} s_1 = 0 \\ s_m = 1 \end{cases} \qquad \text{and} \qquad s_k = \frac{\sum_{j=2}^{k} |\tilde{\boldsymbol{r}}_j - \tilde{\boldsymbol{r}}_{j-1}|}{\sum_{j=2}^{m} |\tilde{\boldsymbol{r}}_j - \tilde{\boldsymbol{r}}_{j-1}|} \quad \text{where} \quad k \in [2, m-1]. \tag{8}$$

where the $\tilde{\boldsymbol{r}}_j$ are the position measurements. In general, solving Eq. (5) with either distribution leads to estimates displaced from the actual measurements, by a value of:

$$d_k = |CM\boldsymbol{s}_k - \tilde{\boldsymbol{r}}_k| \quad k \in [1, m]. \tag{9}$$

where $\boldsymbol{s}_k$ is a vector of all the powers of s_k. Obviously, changing a certain s_k will only affect the value of the corresponding d_k. Thus, it is possible to find a new set of parameters by minimizing a set of aptly chosen cost functions $\{L_k\}$:

$$L_k = (CM\boldsymbol{s}_k - \tilde{\boldsymbol{r}}_k)^{\mathrm{T}}(CM\boldsymbol{s}_k - \tilde{\boldsymbol{r}}_k) \quad k \in [2, m-1] \tag{10}$$

by expanding:

$$L_k = \boldsymbol{s}_k^{\mathrm{T}} MC^{\mathrm{T}} CM\boldsymbol{s}_k - 2\boldsymbol{r}_k^{\mathrm{T}} C\, M\boldsymbol{s}_k + \boldsymbol{r}_k^{\mathrm{T}}\boldsymbol{r}_k \tag{11}$$

Applying the necessary condition for a stationary point leads to a polynomial in s_k:

$$\frac{dL_k}{ds_k} = \frac{dL_k}{d\boldsymbol{s}_k} \cdot \frac{d\boldsymbol{s}_k}{ds_k} = 2\,\boldsymbol{s}_k^{\mathrm{T}} MC^{\mathrm{T}} CM\frac{d\boldsymbol{s}_k}{ds_k} - 2\boldsymbol{r}_k^{\mathrm{T}} C\, M\frac{d\boldsymbol{s}_k}{ds_k} = 0 \tag{12}$$

or equivalently

$$F(s_k) = \boldsymbol{s}_k^{\mathrm{T}} MC^{\mathrm{T}} CM\frac{d\boldsymbol{s}_k}{ds_k} - \boldsymbol{r}_k^{\mathrm{T}} C\, M\frac{d\boldsymbol{s}_k}{ds_k} = 0 \tag{13}$$

Eq. (13) is a polynomial in s_k which can be solved for instance via Newton-Raphson iterations, given an initial guess $\bar{s}_k$:

$$s_k^* = \bar{s}_k - \frac{F(\bar{s}_k)}{F'(\bar{s}_k)} \tag{14}$$

where

$$F'(s_k) = \frac{dF(s_k)}{ds_k} = \frac{d\boldsymbol{s}_k^{\mathrm{T}}}{ds_k} M C^{\mathrm{T}} C M \frac{d\boldsymbol{s}_k}{ds_k} + \boldsymbol{s}_k^{\mathrm{T}} M C^{\mathrm{T}} C M \frac{d^2\boldsymbol{s}_k}{ds_k^2} - \boldsymbol{r}_k^{\mathrm{T}} C\, M \frac{d^2\boldsymbol{s}_k}{ds_k^2} \tag{15}$$

In Eqs. (9 - 15), vector $\boldsymbol{s}_k$ and its derivatives have the following expressions:

$$\boldsymbol{s}_k = \begin{Bmatrix} s_k^n \\ s_k^{n-1} \\ \vdots \\ s_k \\ 1 \end{Bmatrix} \qquad \frac{d\boldsymbol{s}_k}{ds_k} = \begin{Bmatrix} n s_k^{n-1} \\ (n-1) s_k^{n-2} \\ \vdots \\ 1 \\ 0 \end{Bmatrix} \qquad \frac{d^2\boldsymbol{s}_k}{ds_k^2} = \begin{Bmatrix} n(n-1) s_k^{n-2} \\ (n-1)(n-2) s_k^{n-3} \\ \vdots \\ 0 \\ 0 \end{Bmatrix} \tag{16}$$

Minimizing Eq. (10) (note how the first and last point are left unchanged, to ensure the parameter always spans the range $[0, 1]$), leads to a new parameter distribution, that can in turn be used in Eq. (5) to find a new set of control points. To further generalize the method, Eq. (5) can be modified to include measurement weights. Assuming, as is often the case, all measurements to be uncorrelated, the weights matrix W is diagonal. Then:

$$C = R W S^{\mathrm{T}} (S W S^{\mathrm{T}})^{-1} M^{-1} \tag{17}$$

It is immediate to see that Eq. (17) reduces to Eq. (5) when all the weights are equals.

Therefore, the algorithm is constituted of two cycles in sequence: the first, starting at $n = 2$, progressively increases the degree until a local minimum in the average error along the trajectory is found. Once this criterion is met, and the number of control points is established, a second cycle improves on the parameter distribution as explained above. Finally, this optimal distribution is also used to find a best fitting of the measurement times. To summarize, the overall algorithm of the Bézier Least Squares (BLS) is described in Fig. 1.

B. Least Squares for Bézier time description

Analogous to what has been done for position, time along the trajectory can also be expressed as a function of the parameter s. When measurements are taken at constant time steps, the implicit assumption is that t varies linearly with the parameter, as in $t = t_i\,(1-s) + t_f\, s$, which

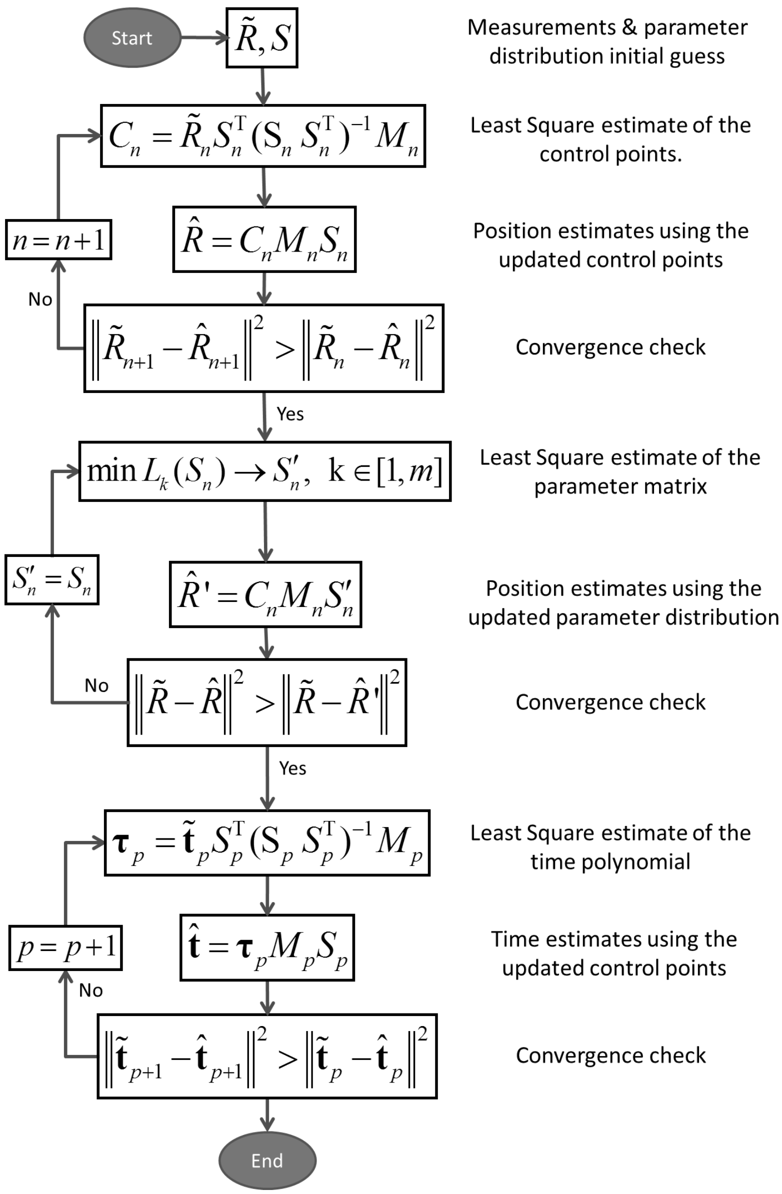

Figure 1. Algorithm scheme.

can be seen as a Bézier function of degree 1. However, velocity variations along the trajectory can be better described with polynomials of higher degree. This degree is generally different from the optimal degree of the interpolated trajectory. The two polynomials exist in different dimensional spaces, with the "time curve" being effectively one dimensional. However, the two are still related via the parameter s, because each measurement is associated with a time instant. Therefore, upon reaching convergence in the estimation of $\boldsymbol{s}_k$, the control points τ for the "time curve" are easily found by applying the same procedure as above:

$$\tilde{\boldsymbol{t}} = \boldsymbol{\tau} M_p S_p \quad \rightarrow \quad \boldsymbol{\tau} = \tilde{\boldsymbol{t}}\, S_p^{\mathrm{T}} \left(S_p S_p^{\mathrm{T}}\right)^{-1} M_p^{-1} \tag{18}$$

where the subscript "p" indicates the degree used in this calculation, which is not necessarily equal to n. Similarly to what is done for position estimation, its value is found by searching for the minimum difference between measured and estimated times:

$$\min_p \, |\tilde{\boldsymbol{t}} - \hat{\boldsymbol{t}}|^2. \tag{19}$$

Because of the monotonic behavior of time, the control points τ_k must satisfy the series of inequalities:

$$t_i < \tau_1 < \cdots < \tau_{n-1} < t_f. \tag{20}$$

It is worth emphasizing that while all of the τ_k are expressed in seconds, they do not represent times of any specific point along the trajectory, but rather, are the control points associated with the time description of the trajectory.

C. Velocity Estimation

As an added result of the method, it is possible to obtain an estimate for the velocity at the measured positions; indeed:

$$\boldsymbol{v}(t) = \frac{d\boldsymbol{r}}{dt} = \left(\frac{d\boldsymbol{r}}{d\boldsymbol{s}}\right)\bigg|_{s_k} \left(\frac{ds}{dt}\right)\bigg|_{s_k} = \left(\frac{d\boldsymbol{r}}{d\boldsymbol{s}}\right)\bigg|_{s_k} \left(\frac{dt}{d\boldsymbol{s}}\right)\bigg|_{s_k}^{-1} \tag{21}$$

Because both $\boldsymbol{r}(s)$ and $t(s)$ are polynomials, these derivatives are extremely simple to find. It is worth noting that Eq. (21) does not return the Bézier function for the velocity (i.e. its control points), but only the estimated velocities at s_k.

III. Bézier Least Squares Sensitivity Analysis

Sensitivity analysis is performed considering a one-dimensional Bézier function. Figure 2 and Figure 3 describe the effect of Gaussian noise in the measurements and convergence of the method when starting with a poor choice of the parameter s, respectively.

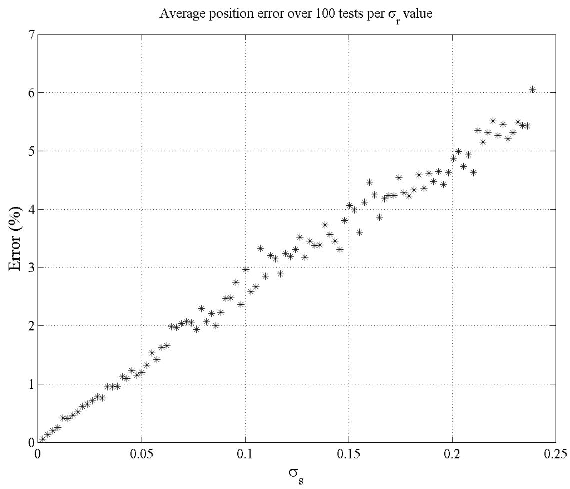

Figure 2. Average error for increasing noise in the measurements.

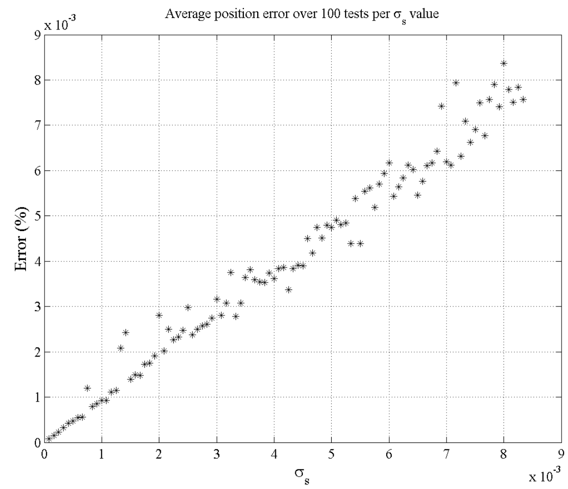

Figure 3. Average error for increasing disturbances in the s distribution.

IV. Numerical tests on Cislunar trajectory

For the estimation of segments of a cislunar trajectory for an Earth-to-Moon mission, the measurements are simulated assuming a camera of focal length 300 mm and random Gaussian noise whose standard deviation is based on the optical properties of the supposed sensor.[1] Weights are introduced by considering the specific geometry at work. Along the trajectory, three segments are considered, close to the Earth, midway, and close to the Moon. Along the first segment the spacecraft is mainly subject to Earth gravitational effects, while along the third the Moon is the principal gravitational body. Each segment consists of 25 measurements, equally spaced over a period of 2 hours. The trajectory is simulated with the GMAT software, taking into account the full gravitational effects of Sun, Earth and Moon, in addition to non-gravitational effects such as solar radiation pressure. The results show the performance of the proposed method point by point along the segments, compared with a Weighted Iterative Least Square (ILS) and an Extended Kalman Filter (EKF), both of which, it is worth reminding, require full state propagation to compute the estimate. For these two methods, the simplified physical model implemented only includes the point mass effects of the Earth and the Moon.

A. Simulation results

For all segments, the ILS reaches convergence after 8 iterations, and the optimal degree found by BLS is 7. As mentioned above, Gaussian noise is superimposed to the simulated measurements. As seen in Figs. (4) to (9), BLS performs comparably with ILS and EKF. Each figure shows the root sum squared of the errors at each measurement time for the three algorithms. The overall performance of the three methods is summarized by taking the average error along each segment in both position and velocity. The results are reported in Table 1.

	Close to Earth	Midway	Close to Moon
ILS Position error (km)	1.4719	0.3519	0.3509
BLS Position error (km)	2.7362	0.6935	0.2212
EKF Position error (km)	1.8694	0.6203	0.3616
ILS Velocity error (km/s)	0.0017	0.0003	0.0003
BLS Velocity error (km/s)	0.0083	0.0022	0.0005
EKF Velocity error (km/s)	0.0108	0.0063	0.0063

Table 1. Average error comparison

It can be seen that the EKF provides progressively worse results as the spacecraft moves further from Earth, while BLS improves. This is mainly due to the fact that EKF (like the ILS) uses a model which does not take into account any perturbation and has zero process noise, therefore its results are less accurate where such perturbations are more prominent. In contrast, BLS only uses measurements and it is "closer" to the truth along segment 3. For this same reason BLS performs better than ILS along segment 3. It is worth noting that even when BLS has a greater margin of error than the other methods, it remains a sensibly simpler method to implement, because it does not require any of the tuning procedures typically associated with the Kalman filters. Moreover, the velocity estimates are obtained very simply as a secondary result according to Eq. (21), while EKF and ILS perform a full state propagation to obtain the same result. Lastly, because of the much simpler mathematics of the BLS, in each case the computational time is roughly one order of magnitude smaller than the one required for EKF and ILS.

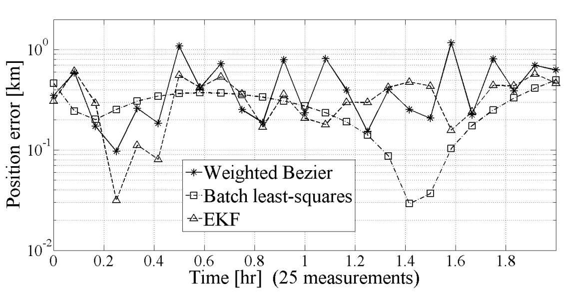

Figure 4. Position estimation error along segment 1. Bézier optimal degree: 7.

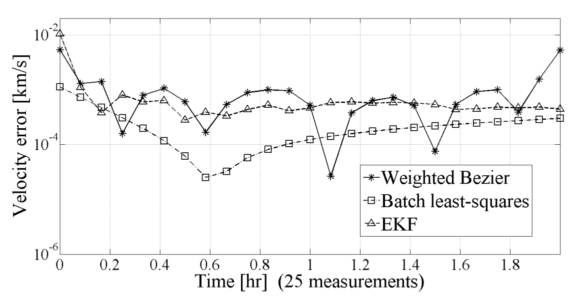

Figure 5. Velocity estimation error along segment 1.

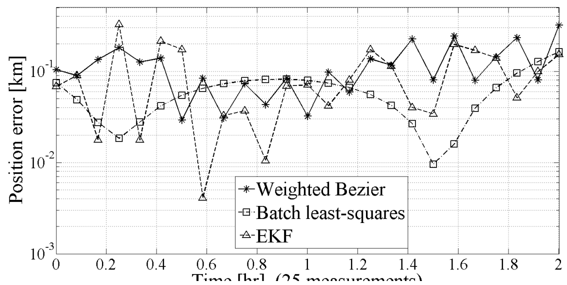

Figure 6. Position estimation error along segment 2. Bézier optimal degree: 6.

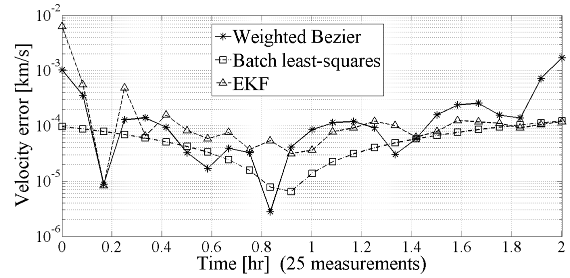

Figure 7. Velocity estimation error along segment 2.

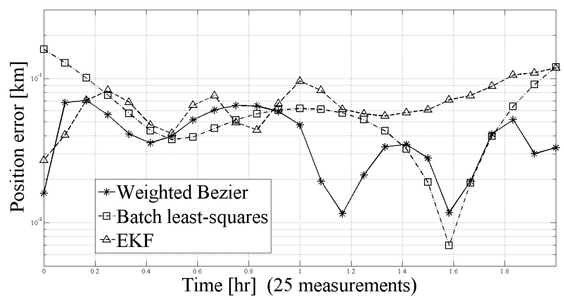

Figure 8. Position estimation error along segment 3. Bézier optimal degree: 7.

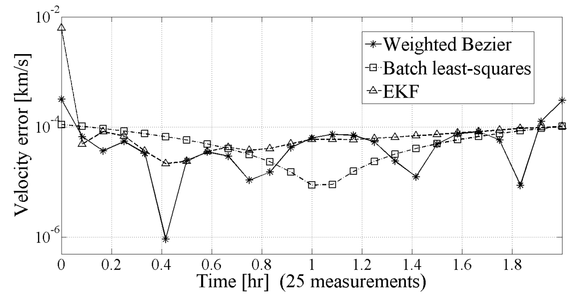

Figure 9. Velocity estimation error along segment 3.

These results suggest that the dynamics is quite perturbed during segment 3 and therefore the EKF could benefit from the addition of process noise. Figs. 10 and 11 show the performance of estimating the trajectory during segment 3 when process noise is added to the EKF with a power spectral density of 1 mm^2/s^2 per axis. It can be noticed that the EKF with and without process noise start out providing similar results but eventually the implementation that includes process noise performs better. BLS and the EKF with process noise provide similar results, however BLS performs slightly better in terms of position error root sum square (0.201 km versus 0.254 km).

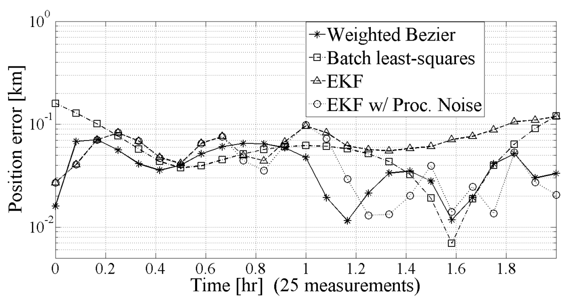

Figure 10. Position estimation error along segment 3 (EKF w. process noise included).

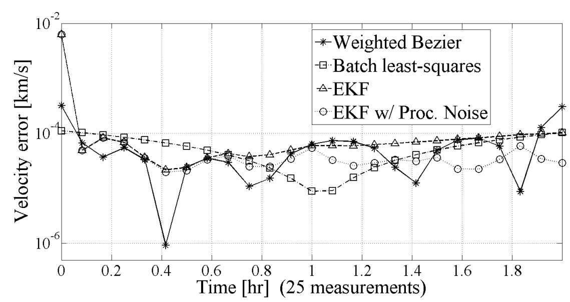

Figure 11. Velocity estimation error along segment 3 (EKF w. process noise included).

V. Conclusions

This work shows that Least Squares applied to Non-Rational Bézier functions provide a reliable approach to describe space trajectories based on a set of measured position vectors. The method has been implemented in an algorithm composed of two main loops, to optimize both the distribution of the implicit parameter s and the degree of the polynomial n. While the latter is limited by numerical instability issues, satisfactory performances are nevertheless achieved thanks to the flexibility of Bézier curves, avoiding the necessity to use polynomials of even higher degree. The proposed approach has been tested in three segments of a simulated cislunar trajectory and compared with iterative Least Squares and extended Kalman filter estimators. The proposed method, simpler in approach and implementation, does not require any dynamical model to work. For this reason it is suitable in those situations where accurate dynamics models are complicate, change often, or are unknown. Since dynamical models are not used, knowledge of process noise and/or dynamical model uncertainty are not needed. Typical examples of such are the solar radiation pressure model (which depends on attitude and solar activity) or venting and accidental pipe leaking events. Compared to other best fitting methods, this approach also provides with velocity estimates, obtained indirectly by interpolating both positions and times rather than directly from velocity measurements.

Numerical test scenarios have been simulated using NASA's "General Mission Analysis Tool" software. Three segments of a cislunar trajectory have been considered. Accuracy results in term of position and velocity estimation are shown to be comparable with those provided by iterative Least Squares and extended Kalman filter estimators. Better performance is shown in the third segment, where the gravitational contribution of the Moon becomes more important. The promising results have encouraged the authors to explore the possibility of using different type of parametric curves, like Rational Bézier Curves and splines, which will be the focus of future research.

Obviously the accuracy obtained using trajectory estimators based on correct dynamical models is certainly better than that obtained using the proposed Least Squares applied to Bézier functions. For this reason the proposed approach is not meant to substitute Kalman filter-type estimators, but it can be used when these estimators need to work far from their nominal (and optimal) range of applicability or when they provide doubtful results. In these cases the proposed method still provides good estimates of both position and velocity.

When the extended Kalman filter is used in a highly uncertain dynamical environment, process noise is used to de-weight the contribution of the prior state to the updated state. In practice this means that both the dynamics model and all of the prior measurements are de-weighted in favor of the current measurement. On the one hand this procedure decreases the estimation error because it does not completely rely on faulty propagation models. On the other hand, however, less information is made available because prior measurements are not completely used. Tuning the process noise is usually an iterative process. The proposed approach is an alternative that does not necessitate tuning and produces comparable results.

References

[1]Mortari, D., de Dilectis, F., and D'Souza, C. "Image Processing of Illuminated Ellipsoid," AAS 13-853, 2013 AAS/AIAA Astrodynamics Specialist Conference, Hilton Head, SC, August 11–15, 2013.

[2]Park, K.J. and Mortari, D. "Planet or Moon Image Processing for Spacecraft Attitude Estimation," *Journal of Electronic Imaging*, Vol. 17, No. 2, April-June 2008, pp. 1-11. DOI: 10.1117/1.2938999.

[3]Gooding, R.H. "A New Procedure for the Solution for the Classical Problem of Minimal Orbit Determination from Three Lines of Sight," *Celestial Mechanics and Dynamical Astronomy.* Vol. 66, No. 1, 1997, pp. 387-423. DOI: 10.1007/BF00049379.

[4]Pastva, T.A. "Bézier Curve Fitting," *Naval Postgraduate School Thesis.* September 1998, Monterey, CA.

[5]Tapley, B.D. et al., *Statistical Orbit Determination*, Elsevier Academic Press, 2004, pp. 199-210.